EPR characterization of Co-doped ZnO microwires and distant spin-pair coupling

Adrien Savoyant, Fabien Giovannelli, F Delorme, A Stepanov

EPR characterization of Co-doped ZnO microwires and distant spin-pair coupling

A. Savoyant,[1] F. Giovannelli,[2] F. Delorme,[2] and A. Stepanov[1]

[1] *IM2NP, CNRS UMR 6242, FST, Aix-Marseille Université, F-13397 Marseille Cedex 20, France*

[2] *Université François Rabelais de Tours, CNRS, CEA, INSA CVL, GREMAN UMR 7347, IUT de Blois, 15 rue de la chocolaterie, CS 2903, 41029 Blois Cedex, France.*

Cobalt-doped ZnO microwires have been grown by the optical furnace method with Co concentration in the range 0–5%. The high crystallinity of these objects is demonstrated by the use of Electron Paramagnetic Resonance (EPR), in which Co^{2+} ions serve as magnetic probes. The spin state of these isolated magnetic impurities and their location in the host crystal are addressed by EPR, as well as the coupling constant between non-nearest Co^{2+}– Co^{2+} neighbors. Eight of these distant spin pairs are detected, among which two are confirmed to be ferromagnetic. The problem of their localization in the wurtzite structure is discussed.

PACS numbers: 61.72.uj, 71.70.Gm, 76.30.Fc

I. INTRODUCTION

As key materials for spintronics and magneto-optical devices, Diluted Magnetic Semiconductors (DMSs) have attracted considerable attention over the past two decades due to the possibility they offer to combine semiconducting and ferromagnetic properties in a single homogeneous material.[1–3] Among a variety of DMSs, ZnO:Co is particulary interesting because of the wide band gap character of ZnO, the highly localized spin of Co impurities and their intense coupling with the host valence bands and lattice.

After a period of controversy, there now exists a large consensus that bulk ZnO:Co displays no intrinsic ferromagnetism[4,5] (ferromagnetism not due to secondary phases or defects). Nevertheless, ZnO-based DMSs continue to be the focus of great interest. Indeed, on the one hand, they are susceptible to be grown in a broad diversity of micro and nano-structures such as wires, cages, rings, etc.[6,7], all of these objects being required by micro and nano-electronics industry, and, on the other hand, the possibility of their co-doping (e.g Co/Fe)[8] is promising. Some devices involving transition-metal-doped zinc oxyde nanostructures already exists, although they do not make use of magnetic properties.[9] Methods for obtaining such low-dimensional objects have then to be tested, regarding the crystal and doping qualities. To this end, Electron Paramagnetic Resonance (EPR) is a tool of choice, being complementary to classical structural probes (such as XRD), in order to demonstrate the crystallinity of an insulating material containing magnetic ions.

Quite often, only single ion EPR spectra can be exploited for proving crystallinity: the g-tensor being anisotropic (a required condition), the resonance fields depend on the relative orientation between the applied magnetic field and the spin environment. These resonance fields then probe the local structure directly around the magnetic impurities and, as a consequence, a small distribution of these fields (i.e narrow EPR lines) indicates a good crystallinity.

More rarely, advantage can be taken from the pair spectra. The main reason is that the common EPR experiment (X-band) can not probe the nearest neighbors (NN) spin pair couplings, which are usually too intense (about ten Kelvin), but only the couplings of distant pairs, which do not exceed 1K (10^{-4}eV). Substantial occurrence of these distant pairs requires a certain concentration of magnetic impurities, which, in turn, implies a large dipolar broadening, rendering the corresponding EPR lines often invisible. Observing such distant spin pairs then requires very high crystallinity: The pair resonance field position (i.e the spin coupling constant) is extremely sensible to the spin-spin separation and orientation, so that narrow pair lines indicate crystal coherence throughout the whole sample, over a length which would be at least of the same magnitude as that between the distant magnetic ions.

In this work, we have studied ZnO:Co microwires (MWs), synthesized by the optical furnace method[10], using EPR at liquid helium temperature. Following the methodology of Ref. [11], we confirm the high crystallinity of these objects through the examination of single and paired ions

EPR spectra. Moreover, we detect eight J exchange constants (fourth to eleventh) between Co magnetic ions are detected and we confirm the presence of two ferromagnetic distant pairs, previously observed in bulk ZnO:Co. The problems of the J's assignment and dipole-dipole contribution to these coupling constants are discussed.

II. METHODS

The Co-doped ZnO powder was synthesized by a solution route.[12] 100 ml of cationic solution was obtained by dissolving $Zn(NO3)_2$,$6H_2O$ (Aldrich, 99.99% purity) and $CoSO_4$ ($Co(NO_3)_2$,$6H_2O$ (Sigma Aldrich, 99 % purity) in demineralized water. The concentration of Zn was 1M and the Co concentration corresponded to 5 at% of the Zn one. The precipitation was performed by the dropwise addition of 50 ml of a 4 mol/l NaOH solution (Labonline micropearls, > 98% purity) during 25 minutes. The obtained precipitate was centrifuged at 4000 rpm during 5 min and washed with demineralized water. This step was repeated five times. The solid was finally dried at 80°C overnight. The resulting powder of Co-doped ZnO, which exhibits a green color, was then placed in a rubber tube and isostatically pressed under 3000 bar. The obtained Co-doped ZnO rod was sintered at 900°C for 10 h in air. This centimeter-long rod, which also shows a green color, was then placed in an optical furnace (Cyberstar). During the experiment, the ZnO bar was rotated at 20 rounds per minute. Well wurtzite-crystallized MWs were obtained in which **c**-axis was parallel to the wire axis: These MWs could reach 300 μm long and exhibited a cross-section ranging from 10 μm up to 100 μm, due to the sublimation of ZnO.[10]
For Co-doped ZnO, two kinds of MWs were observed. The MWs in contact with the surface of the ceramic exhibited a green color gradient, consistent with a diffusion process: Indeed, the basis of the MWs was greener than their apex. This was confirmed by point Energy-Dispersive X-Ray Spectrometry (EDS) analysis performed on MWs (EDS Oxford Inca) in a FEI Quanta 200 Scanning Electron Microscope (SEM). In a MW of 300 micrometers long, the Co atomic concentration measured by EDS was found to decreases from 5 to less than 1 atomic percent. The second kind of MWs was not in contact with the surface and showed a homogeneous pale green color which corresponds to a cobalt concentration lower than 1 atomic percent.
For the EPR study, we have chosen one MW of each type, the diameter of which being about 50 to 80 μm. In this paper, the MW with a homogeneous low Co concentration is called MW1 and the MW with higher heterogeneous concentration is called MW2.

The X-band (ν = 9.39 GHz) EPR spectra were recorded using a Bruker EMX spectrometer equipped with a standard TE_{102} cavity.
A continuous helium-flow cryostat allowed us to reach a temperature of 4.5 K for all recorded spectra. The alignment of the wurtzite **c**-axis (parallel to the MWs axis) with the static magnetic field **B** was controlled by a manual goniometer. As only one angle may be tuned by this goniometer, there could still remain a residual angle between **B** and **c**, which in the following will be referred to as θ angle.
No traces of metallic cobalt inclusion was detected, such as in Ref. [13] ($Zn_{1-x}Co_xO$, with $x = 30\%$), consistently with the low Co-concentration range in our samples MW1 and MW2 ($x < 1\%$, $x \simeq 1-5\%$, respectively).

III. RESULTS

A. Single Ion

The EPR spectra of MW1 and MW2, recorded at 4.5 K around 300 mT, are shown at the top of Fig.1. The eight equally spaced lines are characteristic of a spin 1/2 coupled by hyperfine interaction with an $I = 7/2$ nuclear spin. This is the signature of an isolated Co^{2+} ion ($S = 3/2$) in axial *in-plane* symmetry, for which the ground electronic state is a pseudo-spin 1/2. These lines (derivatives of the field-dependant microwave absorption) correspond to transitions between states separated by $\Delta E = h\nu$ and satisfying the selection rules $\Delta m_S = \pm 1$ and $\Delta m_I = 0$. The spectra of MW1 and MW2 have different gravity centers (B_0) of, respectively, 297.0 mT and 298.5 mT.

Isolated Co^{2+} ions in axial symmetry, subjected to an external magnetic field, are commonly modeled by the following Hamiltonian:

$$H_S = DS_z^2 + \mathbf{S}.\tilde{A}.\mathbf{I} + \mu_B \mathbf{S}.\tilde{g}.\mathbf{B}. \qquad (1)$$

Here, D is the axial zero-field splitting parameter, $\tilde{A}$ the hyperfine tensor and **B** the applied (quasi-) static magnetic field. This latter makes a θ angle with the **z**-axis ($\equiv$ **c**-axis).

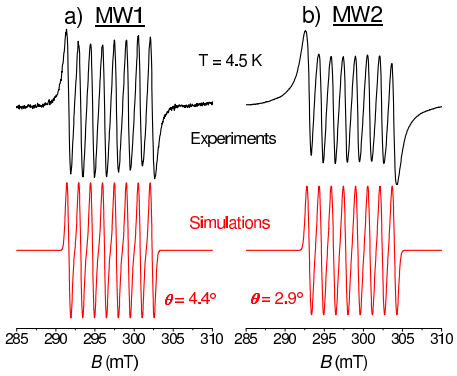

Figure 1: (color online) EPR spectra of ZnO:Co MWs (black, top) with low (MW1) and high (MW2) concentrations of Co^{2+} ions, and the corresponding single ion simulations (red, bottom) from Eq.(1). θ is the angle between static magnetic field **B** and **z** (or **c**) axis entered in the simulation.

For each of these spectra, we first assume that the $\tilde{g}$ tensor has its bulk values, so that the position of the gravity centers are directly linked to the θ angles. We then obtain $\theta = 4.4°$ and $2.9°$ for MW1 and MW2, respectively. These residual angles may arise from any source of misalignment between **z**-axis and **B**. However, they do not affect any of our conclusions since they are included in the simulations.
We then simulate the single-ion spectra with the `EASYSPIN` toolbox.[14] A least-square fitting method allows us to extract the single-ion parameters, reported and compared to those of other ZnO:Co objects in Table I. Due to their weak influence on the lines position, and in order to reduce the number of variables, the D parameter and the perpendicular component of the hyperfine and g tensors have not been adjusted but have been taken to be those of thin films. The adjusted parameters ($A_{\parallel}$ and $g_{\parallel}$) are quite close to those of bulk ZnO:Co. Note that, due to the positive axial anisotropy parameter (D), the spin tends to lay in the hexagonal plane of the wurtzite (W) structure.

The resulting simulations for MW1 and MW2 are shown at the bottom of Fig.1, with gaussian line widths of, respectively, 0.6 and 0.7 mT. Assuming that the resonance-field distribution of a given line (i.e its width) is entirely due to the angular distribution of the spin environment, the simulations show that the observed line widths of MW1 and MW2 correspond to angular distributions of about $\pm 0.3°$ and $\pm 0.4°$, respectively. However, the observed line widths arise from many sources (relaxation, dipole-dipole interaction, etc.), so that angular distributions of the magnetic-ion environment, if any, are certainly very much weaker than these values, which should be seen as upper limits. We can then say that, over the whole crystal, the orientation of the direct spin environment cannot vary by more than a few tenths of a degree.

Compared with the simulated ones, the single-ion spectra display a modulation of the EPR line intensity which cannot be reproduced by a line broadening. This indicates the presence of some additional broad line(s). The modulation having B_0 as symmetry center in both cases, it must reflect a Co-related (Co–Co or Co–crystal) interaction.
Despite these differences, all the line positions are well reproduced by the simulation. This allows us to conclude that the isolated Co impurities are indeed some $S = 3/2$ spins in an axial environment with bulk parameters or, in another words, that Co^{2+} ions effectively substitute Zn^{2+} ones at cationic sites of the W structure.

B. Paired Ions

We now examine in detail the high concentration sample MW2, where pairs of Co^{2+} ions are expected to occur. While the EPR spectrum of MW1 displays lines only in the region 280-310 mT (Fig.1-a), the spectrum of MW2 displays in addition a series of "satellite" and "high-field" broader lines, as shown in the wide-range spectrum (Fig.2). No hyperfine structure is visible in these lines, which have a width of about 5 to 10 mT.
All the satellite lines have $B_0 = 298.5$ mT as gravity center, just as the single-ion lines of MW2. This indicates they are cobalt-related. In this

Table I: EPR single ion parameters for ZnO:Co microwires (MW1, MW2), bulk, and thin film (TF) grown by Molecular Beam Epitaxy (MBE) and Pulsed Laser Deposition (PLD), in 10^{-4} cm^{-1} for $A_{\parallel}$ and in cm^{-1} for D. Error bars for $A_{\parallel}$ and $g_{\parallel}$ of MW1 and MW2 are 0.2×10^{-4} cm^{-1} and 10^{-3}, respectively.

Par.	MW1	MW2	TF(MBE)[4,15]	TF (PLD)[16]	Bulk[17]
$A_{\parallel}$	16.2	16.4	16.1	15.90	16.11
$A_{\perp}$	2.90	2.90		2.90	3.00
$g_{\parallel}$	2.238	2.238	2.236	2.238	2.243
$g_{\perp}$	2.277	2.277	2.277	2.277	2.279
D	2.76	2.76	2.76	2.75	

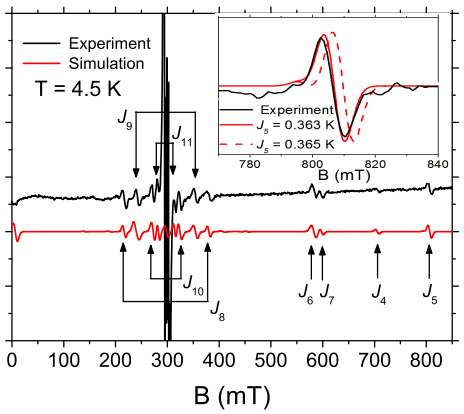

Figure 2: (color online) Wide range X-band spectra of MW2 magnified to make visible the satellite and high-field lines (top,black), and simulation for eight exchange constant (bottom,red). The inset shows the results of fitting of the fifth coupling constant by simulations with $J_5 = 0.363$ K (red solid line), and $J = 0.365$ K (red dashed line), which allow us to estimate the error bars of our data.

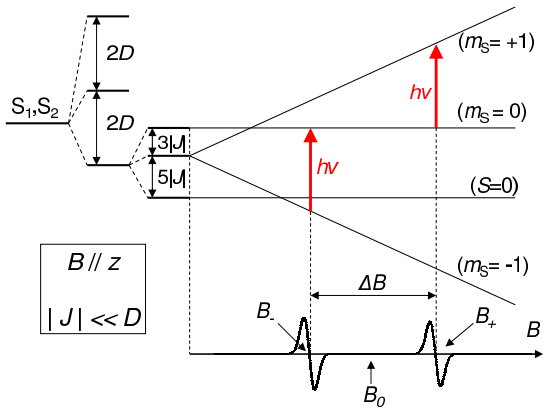

Figure 3: (color online) Level diagram of two $S = 3/2$ spins under uniaxial anisotropy (D), isotropic AFM exchange (J) and magnetic field $\mathbf{B} \parallel \mathbf{z}$, these last two interactions acting only within the ground quartet. EPR transitions ($\Delta S = 0$, $\Delta m_S = \pm 1$) at $h\nu$ are represented by red arrows.

wide-range spectrum, these single-ion lines appear as a big sharp structure around 300 mT (see Fig. 2).

We model the Co^{2+}-Co^{2+} spin interaction by an isotropic Heisenberg Hamiltonian and show that it explains the satellite lines. Considering two spins $S = 3/2$, each one being described by the single-ion Hamiltonian H_S (Eq. 1), the pair Hamiltonian then reads:

$$H_k = H_S(\mathbf{S}_1) + H_S(\mathbf{S}_2) - 2J_k\mathbf{S}_1.\mathbf{S}_2, \qquad (2)$$

where the k index serves to distinguish different kinds of pairs. With this sign convention, $J_k > 0$ (< 0) corresponds to (anti-)ferromagnetic coupling. The Heisenberg interaction is evaluated, to first order, within the ground quartet resulting from the positive axial anisotropy (i.e the $\pm 1/2$ projections of the two $S = 3/2$ spins) and without hyperfine interaction. The splitting diagram of this quartet is shown in Fig.3 for an AFM coupling ($J = -|J|$).

We see that the pair interaction results in a pair of satellite lines around the gravity center B_0, equal to $h\nu/g_\parallel\mu_B$ in this ideal case ($\theta = 0°$). The perturbative treatment of the Heisenberg interaction allows us to express the resonance field of these satellite lines, $g_\parallel\mu_B B_\pm = h\nu \pm 3|J|$, and to simply link them to the corresponding J coupling constant:

$$\Delta B = \frac{6|J|}{g_\parallel \mu_B}. \qquad (3)$$

This formula is equally valid for FM and AFM coupling, provided that $|J| << D$ ($D = 3.97$ K). When $|J|$ exceeds $h\nu/3$ (0.15 K in X-band), the low-field line of the satellite is no longer visible. This explains the observed high-field lines. This formula allows to quickly estimate $|J|$ for given satellite lines.
Note that if the Co^{2+} ions are described by a pseudo-spin 1/2, as in Ref. [23], the axial anisotropy is ignored and is then reintroduced quite artificially in a largely anisotropic exchange tensor, not easily comparable to our J constant.
To simulate the wide-range spectra of MW2, we perform an exact diagonalization of the pair Hamiltonian H_k within the whole state space (two spins 3/2) with the `EASYSPIN` toolbox.[14] This allows us to take into account the small residual angle as well as the slight influence of the axial anisotropy (D) on the position of the satellite lines.

Assuming that all distant pair have the same probability to occur (bulk case), each of the pair Hamiltonians (2) is simply weighted by the experimental pair's coordination number z_k given in Ref. [11] for bulk ZnO:Co. We have then only adjusted the intensity of each coupling constant J. The resulting simulation is shown at the bottom of Fig. 2 and displays an overall good agreement for $k = 4$ to 11. All the simulated pair spectra include the same single ion parameters (and in particular

the θ angle, specific to the MW2 sample), so that the closeness of the resulting J values to the bulk ones (see Tab. II) makes the present modeling very convincing.

The main discrepancies are the slightly underestimated intensity of J_7 and J_8, and the position and width of the zero-field line (ZFL). This first point certainly reflects a difference between the numbers of J_7 and J_8 pairs compared with those observed in bulk: Indeed, it can be avoided by slightly increasing the weight of these pairs (or slightly decreasing the weight of all the others). The second point may be due to a baseline effect combined with broad lines from other clusters, such as triplets or so.

Table II: Left part: J labeling, bulk J values[11], and MW2 J values (in K). Right part: Pair labeling, distance (in Å) and coordination number.

J_k	Bulk[11]	MW2	P_i	R_i	z_i
J_1	-25.6		P_1	3.21	6
J_2	-8.5		P_2	3.25	6
J_3	-1.070		P_3	4.57	6
J_4	-0.382	-0.379 ± 0.002	P_4	5.20	2
J_5	$+0.347$	$+0.363 \pm 0.002$	P_5	5.60	12
J_6	$+0.168$	$+0.170 \pm 0.001$	P_6	5.63	6
J_7	-0.134	-0.138 ± 0.001	P_7	6.13	12
J_8	-0.040	-0.041 ± 0.001	P_8	6.50	6
J_9	-0.027	-0.028 ± 0.001	P_9	7.25	12
J_{10}	$\|0.013\|$	$\|0.013\| \pm 0.001$	P_{10}	7.66	12
J_{11}		$\|0.008\| \pm 0.001$	P_{11}	7.94	6

Despite these discrepancies, the simulation allows to reproduce all the observed resonance fields and to deduce the corresponding J coupling constants, which are reported in table II. We see that these constants are very close to those previously measured in bulk and that we can observe an additional coupling (J_{11}) which was not resolved before. Quite interestingly, the two ferromagnetic pairs found in bulk (J_5, J_6) are also observed in our sample, with almost the same coupling constant.
The inset of Fig. 2 illustrates the estimation of error bars given in Tab. II. They mainly includes the deviation originating from baseline effects.

IV. DISCUSSION

We begin to discuss the crystal quality inferred from the examination of pair spectra. The simulations show that the pair resonance field which is the most sensitive to the relative orientation between the magnetic field and the pair is J_5, which has a line width of roughly 6 mT. As in Sec. III A, we assume that the only source of this broadening is a distribution in pair orientation, and deduce that this distribution cannot exceed $\pm 0.3°$ around the θ value (2.9° for MW2). However, there are many causes of broadening apart from the angular distribution, so that this latter must be substantially smaller than $\pm 0.3°$. This argument is in fact even more true for the pair lines because the unresolved hyperfine interaction largely contributes to the line width of $\sim$ 6 mT. As a consequence, the observation of pair lines reduces even more the maximum value of the angular distribution, as compared with the one deduced from single-ion lines.
Another source of broadening can be a distribution in the J value: The coupling constant being dependent on R (distance between magnetic ions), a distribution of the J value may reflect a distribution in the lattice parameters. For a distant Mn-Mn pair in the zinc-blende structure, the R-dependence of J was experimentally found to be $R^{-6.8}$ (based on spin-glass transition[18]) and theoretically to be $R^{-8.5}$ (superexchange calculation[19]). Extrapolating these results to Co-Co pairs in the W structure, we deduce from the J_5 line width that the distribution of R cannot exceed ± 0.1 %.
Quantitative results for these maximum angular and lattice-parameter distributions would require to quantitatively and exhaustively take into account all sources of broadening. This task is beyond the scope of this paper where we simply emphasize the relation between the observation of pair lines and the sample crystallinity, and conclude that the angular and lattice-parameter dispersion can not exceed 0.3° and 0.1%, respectively.
We now remark that in MW2, and quite unusually, pair lines are observed together with the single ion ones. Indeed, in the case of homogeneous doping, the magnetic-impurity concentration necessary to observe pair lines usually implies a large dipolar broadening in the single ion spectra, making its hyperfine structure unresolved.[15] The observation of both resolved-pair and single-ion lines in the spectra of MW2 can be explained by the doping inhomogeneity, due to the diffusion process: while a pair signal appears with line width augmented by the greater number of magnetic impurities in its vicinity, there still exists large region(s) where Co^{2+} ions remain quite isolated and not subject to this dipolar broadening.

This inhomogeneity in the magnetic-impurity repartition does not allow us, unfortunately, to use a statistical model to relate concentration and pair/single ratio. The statistical model for evaluating single, pair and triplet probability derived by Behringer[20] (and used by Ney *et al.*[21,22] in the same system) considers that an impurity in the W structure is isolated if these 12 nearest-neighbor cationic sites are unoccupied by other impurities. Clearly, this model is not relevant in our case where pairs of distant neighbors are detected. We then simply assume that the probability for a pair to occur is equal to its coordination number (z), that is the number of pairs equivalent to it.
This leads us to some consideration about pair classification. Following Shapira *et. al*[24], we group pairs in equivalent classes, and arrange these latter by increasing distance. For a compressed W structure (ZnO case), the six first classes of pairs are displayed in Fig. 4. This classification is unambiguous for a given structure but not in general cases: for an elongated W structure, $R_1 > R_2$ (and $R_5 > R_6$), whereas for an ideal one, $R_1 = R_2$ (and $R_5 = R_6$).
To this enumeration of pairs by classes, we add the distinction that some of them have the two Co^{2+} ions in equivalent positions (A-A type) and some other have not (A-B type). In a A-A pair, the nearest-neighbor tetrahedrons of each Co^{2+} ion have the same orientation, whereas in a A-B one, they are rotated by 60 degrees.[25]

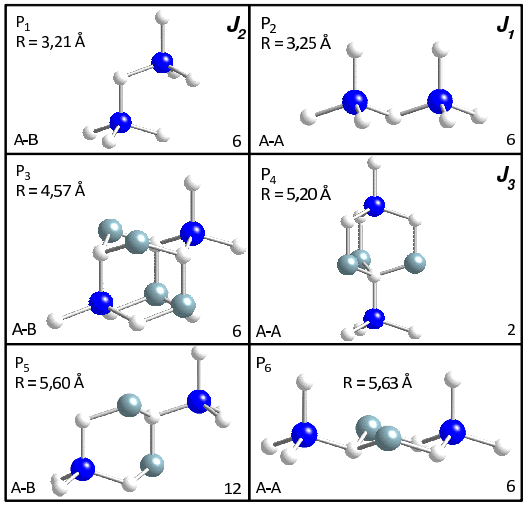

Figure 4: (color online) The first six classes of Co^{2+}-Co^{2+} pair in the W structure. For each of them, the distance (R), the coordination number (z) and the pair type (A-A or A-B) are indicated. In light gray, gray, and blue are represented, respectively, the oxygen, the zinc and the cobalt ions.

We now turn to the discussion about the spin coupling values. Regarding the obtained J values, the closeness of these to the bulk ones indicates a robust property (independent of growing and doping methods) of Co^{2+} in bulk ZnO. The full justification of the sign of all constants requires a combination of different experiments as described in Ref. 11. Here, we have just entered in the simulation the signs obtained in Ref. 11 and we observe that this well reproduces the experimental spectra with almost bulk values.
From a practical point of view, and compared with other magnetic probes applied on ZnO:Co epitaxial thin films such as SQUID or XMCD[21,22] (which result in a $M(B)$ curve), EPR offers a unique way to obtain accurate weak J couplings, and to access the hyperfine structure anisotropy. This latter property being certainly influenced by the confinement in one or more dimension, it could serve as a characterization property for ZnO:Co nanostructures.
We now discuss the problems of dipole-dipole contribution and pair assignment, which are linked together. Given a certain J constant, a known difficulty is that of assigning it a particular class of pair (P_i). This, which is interest by itself, makes furthermore impossible to precisely evaluate the dipole-dipole contribution to the Co^{2+}-Co^{2+} coupling and, as a consequence, the exact contribution of the exchange coupling. In spite of this, J_1, J_2 and J_3 may have been assigned (by consideration on coordination number and superexchange calculation[25]) to P_2, P_1 and P_4, respectively. The problem is then to go on making a univocal correspondence between the J_k's and the P_i's. Clearly, this is a difficult task but we can at least say that the next J should correspond to some pairs of 5 to 8 $\AA$ of distance, for which dipole-dipole interaction may be approximated by $(g\mu_B)^2/r^3 = 20$ to 5 mK, respectively. The given J values which are in this order of magnitude (J_8 to J_{11}) have then to be interpreted as *effective* exchange coupling, which are in reality composed of exchange and dipolar contributions.
Dipole-dipole contributions being anisotropic, angular-dependent EPR could theoretically give some elements of response but, actually, the shift of satellite lines with angle between $\mathbf{B}$ and $\mathbf{z}$ cannot be followed because these lines rapidly collapse into a big broad line. The angle dependence of high-field lines can be followed but, due to the weakness of the dipole-dipole contribution in these, no deviation from isotropic exchange-like coupling can be detected so that no discrimination between hypothetical P_i can be made. In fact, X-band EPR is

not the appropriate tool for obtaining such precise geometrical information: while EPR is sensitive to extremely small energy splittings, its wavelength of a few centimeters is far too big to probe such fine structural details. The use of angular-dependent neutron scattering, with the appropriate wavelength, would probably allow us to discriminate between different pairs.

This problem of the J assignment is of particular importance regarding J_5 et J_6, the two ferromagnetically coupled pairs. To understand the coupling sign of these pairs by a quantitative model, the precise knowledge of their position in the W lattice is required. However, the problem could be inverted: a calculation which would predict the sign and magnitude of the coupling constant as a function of pair position in the lattice would be likely to make an unambiguous correspondence.[26] If the pairs corresponding to J_5 and J_6 can be clearly determined, it can be envisaged to increase their occurrence, thereby reducing the global AFM coupling. Such an increase of the occurrence of J_5 and J_6 would be seen in EPR spectra by an increase of the intensity of the corresponding lines.

Even apart from the assignment of J_5 and J_6, it would be very interesting to investigate by EPR some ZnO:Co nanowires grown along various crystallographic directions, in order to observe a decrease in the occurrence of the pairs lying in the reduced dimensions, and possibly partially answer the assignment problem. This would require an array of perfectly aligned nanowires, grown on a diamagnetic substrate.

V. CONCLUSION

EPR of ZnO:Co MWs has allowed us to reach a double objective: (1) proving the crystallinity of such micro-objects, thus validating the optical furnace growth method, and (2) probing the spin coupling constant between pairs of distant Co^{2+} ions.

First, by detecting from isolated magnetic ions to more and more distant paired ones, EPR proves that the sample under consideration is the repetition of identical bigger and bigger clusters. The quality of this repetition is related to the EPR line width in a complicated manner, but, the simple fact of observing these pair lines indicates a high crystallinity. The optical furnace method is therefore validated as a new route for designing ZnO-based micro- and nano-objects.

Second, we confirm the spin coupling constant values previously observed in bulk ZnO:Co, which then appear as robust properties of paired cobalt ions in ZnO. Two of these constants are found to be ferromagnetic, and we draw the reader's attention to the interesting problem of univocally assigning them to some specific pairs in the W structure.

We conclude that the optical furnace method is an efficient and easy technique to synthesize doped single crystalline ZnO for EPR measurements, which allows one to overcome the difficult and long crystal growth step. Therefore, this synthesis route will allow researchers to explore the properties of various doped ZnO samples to get the spin state and the coupling constants for each dopant. Finally, we suggest that ZnO:Co nanowires could be a pertinent option for increasing the relative occurrence of the pairs lying along the wire-axis, provided that the confinement within the wire section be sufficient in order to reduce the occurrence of the other ones.

VI. ACKNOWLEDGEMENT

A. Savoyant ackownledge financial support from the North Atlantic Treaty Organization (Belgium) project SFP-984735.

[1] H. Ohno, Science **281**, 951 (1998).
[2] I. Žutić, J. Fabian, and S. Das Sarma, Rev. Mod. Phys. **76**, 323 (2004).
[3] T. Dietl, Phys. Rev. B **77**, 085208 (2008).
[4] P. Sati, R. Hayn, R. Kuzian, S. Régnier, S. Schäfer, A. Stepanov, C. Morhain, C. Deparis, M. Laügt, M. Goiran, and Z. Golacki, Phys. Rev. Lett. **96**, 017203 (2006).
[5] A. Ney, K. Ollefs, S. Ye, T. Kammermeier, V. Ney, T. C. Kaspar, S. A. Chambers, F. Wilhelm, and A. Rogalev, Phys. Rev. Lett. **100**, 157201 (2008).
[6] Z. L. Wang, Mater. Sci. Eng. R **64**, 33 (2009).
[7] A. B. Djurisic, A. M. C. Ng, and X. Y. Chen, Prog. Quantum Electron **34**, 191 (2010).
[8] S. Ghosh,Q. Wang, G. P. Das, and P. Jena, Phys. Rev. B **81**, 235215 (2010).
[9] C. O. Chey, X. Liu, H. Alnoor, O. Nur, and M. Wilander (2015) Phys. Status Solidi RRL, 9:87-91.
[10] F. Giovannelli, G. Rajonson, J. Wolfman, and F. Delorme, Materials Letters **107**, 194 (2013)
[11] S. D'Ambrosio, V. Pashchenko, J.-M. Mignot, O. Ignatchik, R. O. Kuzian, A. Savoyant, Z. Golacki, K.

Grasza, and A. Stepanov, Phys. Rev. B **86**, 035202 (2012).
[12] F. Giovannelli, A. Ngo Ndimba, P. Diaz-Chao, M. Motelica-Heino, P. I. Raynal, C. Autret, and F. Delorme, Powder Technology **262**, 203 (2014).
[13] H. J. von Bardeleben, N. Jedrecy, and J. L. Cantin, Appl. Phys. Lett. **93**, 142505 (2008).
[14] S. Stoll, and A. Schweiger, J. Magn. Reson. **178**, 42 (2006).
[15] P. Sati, A. Stepanov, and V. Pashchenko, Low Temp. Phys. **33**, 927 (2007).
[16] N. Jedrecy, H. J. von Bardeleben, Y. Zheng, and J.-L. Cantin, Phys. Rev. B **69**, 041308 (2004).
[17] T. Estle, M. De Wit, Bull. Am. Phys. Soc. **6**, 445 (1961).
[18] A. Twardowski, H. J. M. Swagten, W. J. M. de Jonge, and M. Demianiuk, Phys. Rev. B **36**, 7013 (1987).
[19] T. M. Rusin, Phys. Rev. B **53**, 12577 (1996).
[20] B. E. Behringer, J. Chem. Phys. **29**, 537 (1958).
[21] A. Ney, T. Kammermeier, K. Ollefs, S. Ye, V. Ney, T. C. Kaspar, S. A. Chambers, F. Wilhelm, and A. Rogalev,
[22] A. Ney, V. Ney, F. Wilhelm, A. Rogalev, and K. Usadel, Phys. Rev. B **85**, 245202 (2012).
[23] D. V. Azamat, A. Dejneka, V. A. Trepakov, L. Jastrabik, M. Fanciulli, V. Y. Ivanov, M. Godlewski, V. I. Sokolov, J. Rosa, and A. G. Badalyan, Phys. Status Solidi RRL **5**, 138 (2011).
[24] X. Gratens, V. Bindilatti, N. F. Oliveira, Y. Shapira, S. Foner, Z. Golacki, and T. E. Haas, Phys. Rev. B **69**, 125209 (2004).
[25] A. Savoyant, S. D'Ambrosio, R. O. Kuzian, A. M. Daré, and A. Stepanov, Phys. Rev. B **90**, 075205 (2014).
[26] Current *ab initio* calculations have not enough energetic precision to solve the problem of the coupling between distant neighbors, which is of the order of some 10^{-5} eV or less. Analytical calculations based on model Hamiltonians are then required.